

*Hee-Jong Choi*  
*Hyun-Sik Yoon*



<http://dx.doi.org/10.21278/brod67301>

ISSN 0007-215X  
eISSN 1845-5859

## RESEARCH ON HULL-FORM OPTIMIZATION OF A PASSENGER SHIP USING HULL-FORM MODIFICATION ALGORITHM WITH GAUSSIAN DISTRIBUTION FUNCTION

UDC 629.5(05) 629.541.4:629.5015.24:519.61

Original scientific paper

### Summary

The present study proposes an automatic hull form control algorithm to effectively control the hull form of a ship. A Gaussian distribution function is implemented in the proposed algorithm that automatically controls the hull form in conjunction with an optimization algorithm that is executed during the hull form optimization procedure. The hull form optimization algorithm adopts sequential quadratic programming for the optimizer, and the wave-making resistance is used as an objective function and is solved using the potential-based panel method. A high-speed passenger ship is selected as the target ship, and the results of a numerical analysis of the original hull are compared to those of the optimized hull obtained using the hull form optimization in order to verify the effectiveness of the hull-form optimization technique using the proposed automatic hull form control algorithm.

*Key words:* *Hull-form modification; Hull-form optimization; Gaussian distribution function; Passenger ship; Potential-based panel method; Sequential quadratic programming; Wave-making resistance*

### 1. Introduction

The most important element to improve competitiveness in ship design, is to reduce costs, and a core issue for cost reduction is to improve energy efficiency. Thus, energy efficiency and hull form design are closely associated with cost savings.

The hull form design procedure generally consists of the selection of a mother ship, modification of the mother ship according to changes in the ship specification and verification of the modified hull form via experimental fluid dynamics (EFD) or computational fluid dynamics (CFD). Research on the selection of the mother ship and verification via EFD or CFD have already shown much progress. Modifying the mother ship is always a challenge and subject to research [6, 7].

In recent years, the computational speed of both software and hardware has noticeably developed, and as a result, several interesting research papers have been published on the application of optimization algorithms to hydrodynamic hull form design. Three core technologies that have been applied to hydrodynamic hull form optimization include geometric modeling, hydrodynamic analysis, and optimization techniques. For these technologies to be properly applied to ship design, a sufficient understanding of each technique is required [3, 5, 8, 10, 11, 12].

During hull-form optimization, the hull-form of a ship automatically changes dozens of times or even hundreds of times during a satisfactory hull-form is maintained. Therefore, it is very important to apply a reliable, automatic method to control the hull-form.

The present study proposes an automatic hull form control algorithm that can efficiently control the hull form of a ship. A Gaussian distribution function is applied to the proposed algorithm designed to automatically control the hull form in conjunction with the optimization algorithm used for the hull form optimization procedure. Sequential quadratic programming (SQP) is adopted as an optimizer in the hull form optimization algorithm, and the wave-making resistance is used as an objective function and is solved using the potential-based panel method in which fully non-linear free surface conditions and the panel cutting method are used to generate the computational panels for the hull. A high-speed passenger ship is selected as the target ship, and the results of the numerical analysis for the original hull are compared to those of the optimized hull that was obtained by performing hull form optimization in order to verify the effectiveness of the hull-form optimization technique using the proposed automatic hull form control algorithm.

## 2. Control of hull-form geometry

During hull-form optimization, the hull-form of a ship should be automatically changed dozens of times or even hundreds of times and the modified hull-form must maintain a satisfactory hull-form. Therefore, it is very important to apply a reliable method to effectively control the hull-form. In the present study, an automatic hull-form control algorithm has been proposed by adopting a Gaussian distribution function [1].

### 2.1 Control of a hull profile

In the hull-form control algorithm presented here, the hull profile is modified first. A Gaussian distribution function was adopted to effectively control the hull profile, as shown in Fig. 1, and the related formula is represented using Eq. (1).

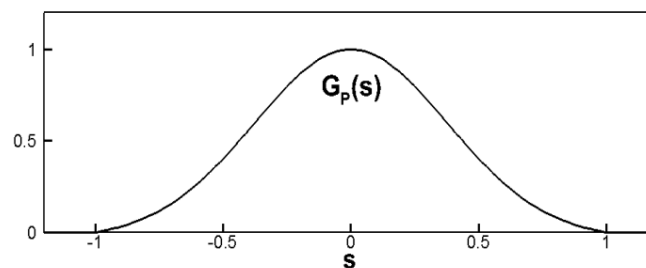


**Fig. 1** Gaussian distribution function adopted to control the hull profile

$$G_p(s) = e^{-3.5s^2} - |s|e^{-3.5} \quad (1)$$

Fig. 2 illustrates an example of the hull profile modification. As shown in Figs. 2 and 3, the original hull profile (solid line, black) is moved to the modified hull profile (dashed line, red). The grid point ( $s = 0$ ) is moved  $\alpha$  meters in the direction of the normal vector of the original hull profile ( $\vec{n}_i^0$ ), and the grid points near the grid point ( $s = 0$ ) are moved  $\alpha G_P(s)$  meters to the normal vector direction of the original hull profile ( $\vec{n}^0$ ) while  $\alpha$  is used as a design variable in the present optimization problem.

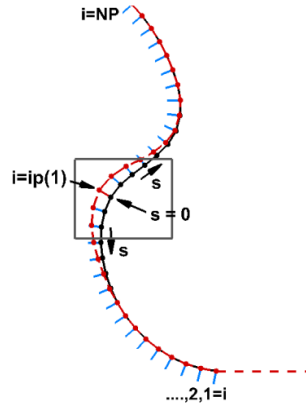


**Fig. 2** Description of the design variables and parametric distance ( $s$ ) and normal vector to control the hull profile

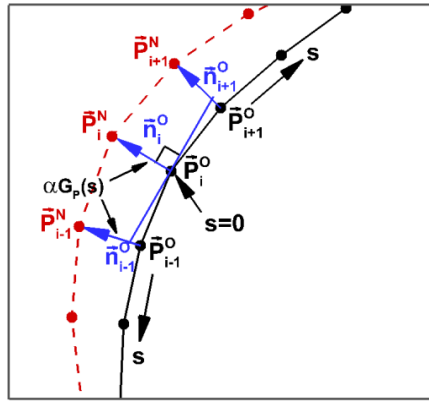


**Fig. 3** Zoom in of the rectangular part of Fig. 1

The relation between the original grid points ( $\vec{P}^0$ ) and the modified grid points ( $\vec{P}^N$ ) can be represented by Eq. (2).

$$\vec{P}_i^N = \vec{P}_i^0 + \sum_{k=1}^{k=NDP} \alpha_j G_P \left( s_i^{ip(k)} \right) \vec{n}_i^0, i = 1, 2, \dots, NP \quad (2)$$

$\vec{P}_i^0 = (xp_i^0, yp_i^0, zp_i^0)$  : Geometry of the original hull

$\vec{P}_i^N = (xp_i^N, yp_i^N, zp_i^N)$  : Geometry of the modified hull

$\vec{n}_i^0 = (n_{x_i}^0, n_{y_i}^0, n_{z_i}^0)$  : Normal vector of  $i$ -th grid point

$G_P \left( s_i^{ip(k)} \right)$  : Gaussian distribution function

$\alpha_k$ : k-th design variable

$NDP$  : Number of the design variables

$NP$  : Number of the grid points

$ip(k)$  : Location of the k-th design variable

$$s_i^{ip(k)} = 4 \sum_{j=i+1}^{j=ip(k)} \sqrt{(xp_j - xp_{j-1})^2 + (zp_j - zp_{j-1})^2} / s_{max} , i \leq ip(k)$$

$$s_i^{ip(k)} = 4 \sum_{j=ip(k)+1}^{j=i} \sqrt{(xp_j - xp_{j-1})^2 + (zp_j - zp_{j-1})^2} / s_{max} , i > ip(k)$$

$$s_{max} = \sum_{j=2}^{j=NP} \sqrt{(xp_j - xp_{j-1})^2 + (zp_j - zp_{j-1})^2}$$

Fig. 4 provides an example of the hull profile modification when 2 design variables have been used. The first design variable ( $ip(1)$ ) is +1 meter to the normal vector direction of the original hull profile, and the second design variable ( $ip(2)$ ) is -1 meter to the normal vector direction of the original hull profile.

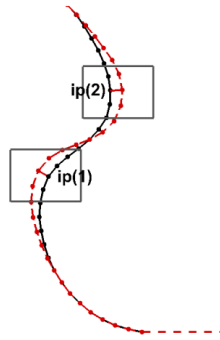


Fig. 4 Modification of the hull profile using 2 design variables

### 2.2 Control of the hull surface

After the hull profile has been modified, the grid points constituting the grid net are moved along the modified hull profile. The grid net of the original hull in Fig. 5 (a) could be mapped directly onto the rectangular grid net, as shown in Fig. 5 (b), since the hull surface grid is generated in a structured form.

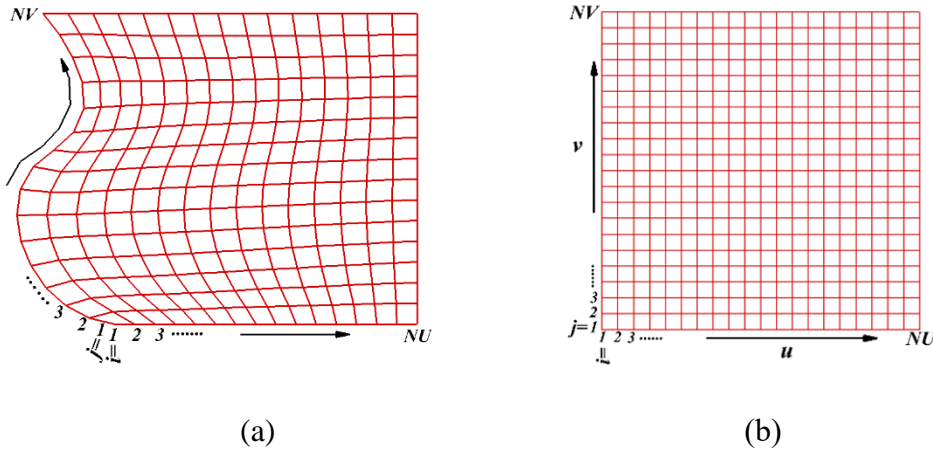


Fig. 5 Mapping from the hull grid net to the rectangular grid net

The grid points located in the boundaries are first changed according to the modified hull profiles shown in Fig. 4 and then the grid points inside the boundaries are changed and this grid transformation process is achieved by applying Eqs. (3)-(6).

$$x_{i,j}^* = x_{i,j}^O + (1 - c_u)(x_{1,j}^N - x_{1,j}^O) + c_u(x_{NU,j}^N - x_{NU,j}^O) \quad (3)$$

$$x_{i,j}^N = x_{i,j}^* + (1 - c_v)(x_{i,1}^N - x_{i,1}^*) + c_v(x_{i,NV}^N - x_{i,NV}^*) \quad (4)$$

$$z_{i,j}^* = z_{i,j}^O + (1 - c_u)(z_{1,j}^N - z_{1,j}^O) + c_u(z_{NU,j}^N - z_{NU,j}^O) \quad (5)$$

$$z_{i,j}^N = z_{i,j}^* + (1 - c_v)(z_{i,1}^N - z_{i,1}^*) + c_v(z_{i,NV}^N - z_{i,NV}^*) \quad (6)$$

$$c_u = (e^{u_{i,j}} - 1)/(e - 1)$$

$$c_v = (e^{v_{i,j}} - 1)/(e - 1)$$

$$u_{1,j} = 0$$

$$u_{i,j} = u_{i-1,j} + \sqrt{(x_{i,j}^O - x_{i-1,j}^O)^2 + (z_{i,j}^O - z_{i-1,j}^O)^2}$$

$$u_{i,j} = u_{i,j}/u_{NU,j}$$

$$v_{i,1} = 0$$

$$v_{i,j} = v_{i-1,j} + \sqrt{(x_{i,j}^O - x_{i,j-1}^O)^2 + (z_{i,j}^O - z_{i,j-1}^O)^2}$$

$$u_{i,j} = u_{i,j}/u_{i,NV}$$

$$i = 2, \dots, NU - 1$$

$$j = 2, \dots, NV - 1$$

$x_{i,j}^O, z_{i,j}^O$  : Geometry of the original hull

$x_{i,j}^N, z_{i,j}^N$  : Geometry of the modified hull

$NU$  : Number of the grid points in u-direction

$NV$  : Number of the grid points in v-direction

Fig. 6 shows the original grid net (black lines) and the modified grid net (red lines).

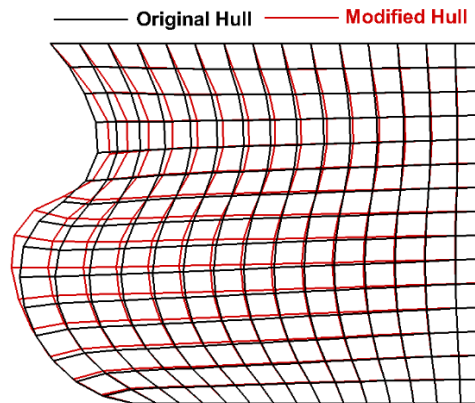


**Fig. 6** Modification of the grid net

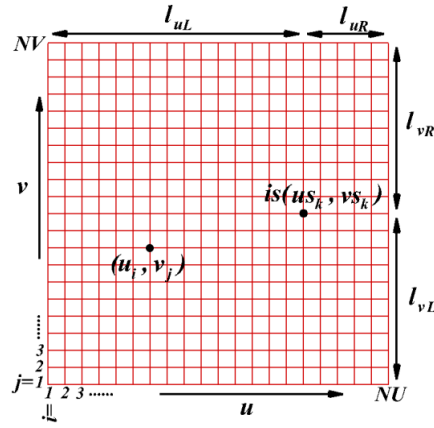


**Fig. 7** Description of the design variables and the rectangular grid net used to control the hull surface

In Fig. 7,  $is(u_{s_k}, v_{s_k})$  is a design variable that is used to control the hull surface in the rectangular grid net. In the horizontal direction,  $l_{uL}$  is the length between  $u_1$  and  $u_s$ ,  $l_{uR}$  is the length between  $u_s$  and  $u_{NU}$ . In the vertical direction,  $l_{vL}$  is the length between  $v_1$  and  $v_s$ ,  $l_{vR}$  is the length between  $v_s$  and  $v_{NV}$ .

A Gaussian distribution function is effectively applied in order to control the hull surface, as shown in Fig. 8, and the related formula is represented using Eq. (7).

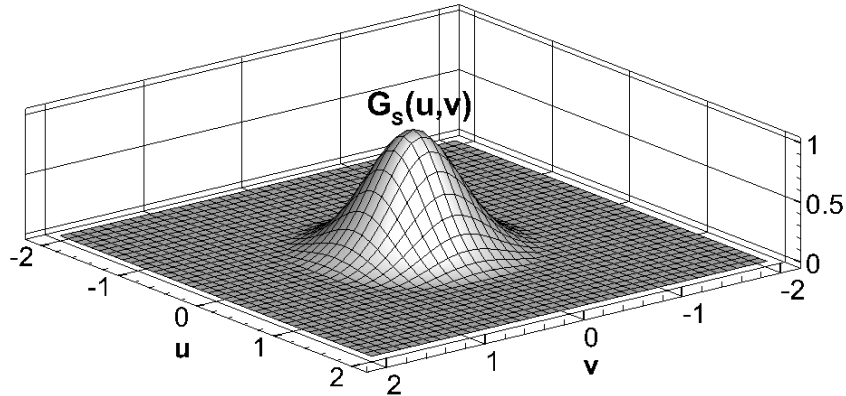


**Fig. 8** Gaussian distribution function used to modify the hull surface

$$G_S(u, v) = [e^{-3.5 u^2} - |u|e^{-3.5}] [e^{-3.5 v^2} - |v|e^{-3.5}] \tag{7}$$

The relation between the original grid points and the modified grid points can be represented using Eq. (8).

$$y_{i,j}^N = y_{i,j}^O + \sum_{k=1}^{k=NDS} \alpha_k G_S \left( \xi_i^{is(u_{s_k}, v_{s_k})}, \eta_j^{is(u_{s_k}, v_{s_k})} \right), \tag{8}$$

$i = 1, 2, \dots, NU, \quad j = 1, 2, \dots, NV$

$y_{i,j}^O$  : Geometry of the original hull

$y_{i,j}^N$  : Geometry of the modified hull

$G_s(\xi_i^{is(us_k, vs_k)}, \eta_j^{is(us_k, vs_k)})$ : Gaussian distribution function

$$\xi_i = \begin{cases} (u_i - us_k)/l_{uL} & \text{if } u_i \leq us_k \\ (us_k - u_i)/l_{uR} & \text{if } u_i > us_k \end{cases}, i = 1, 2, \dots, NU$$

$$\eta_j = \begin{cases} (v_j - vs_k)/l_{vL} & \text{if } v_j \leq vs_k \\ (vs_k - v_j)/l_{vR} & \text{if } v_j > vs_k \end{cases}, j = 1, 2, \dots, NV$$

$NDS$  : Number of the design variables used to modify the hull surface

$is(us_k, vs_k)$  : Location of the k-th design variable  
used to modify the hull surface

Fig. 9 shows the location of the design variables. Fig. 10 compares the original hull and the modified hull after applying only 1 design variable ( $is(us_1, vs_1)$ ) and Fig. 11 compares the original hull and the modified hull after applying 2 design variables ( $is(us_1, vs_1)$  and  $is(us_2, vs_2)$ ).

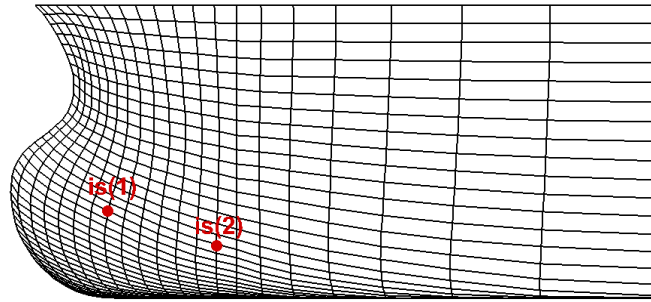
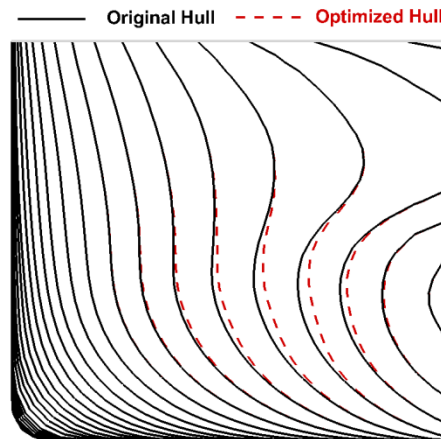
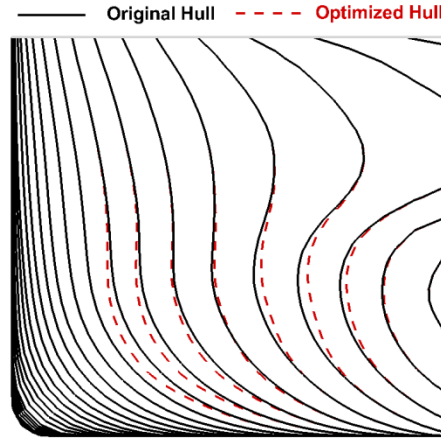


**Fig. 9** Location of the design variables



$is(us_1, vs_1)$  is moved -1 meter in the transverse direction

**Fig. 10** the original hull and the modified hull after applying 1 design variable ( $is(us_1, vs_1)$ )



$is(us_1, vs_1)$  and  $is(us_2, vs_2)$  are moved -1 meter and +1 meter in the transverse direction

**Fig. 11** the original hull and the modified hull after applying 2 design variable ( $is(us_1, vs_1), is(us_2, vs_2),$ )

### 3. Optimization algorithm

The optimization algorithm plays an important role in the hull-form optimization problem. The hull-form optimization problem consists of design variables, constraint conditions and an objective function, and the design variables in the hull-form optimization problem are mainly used to control the geometry of a ship while the constraint conditions are the values by which the design variables are restricted. The objective function that is minimized or maximized during the optimization procedure is a criterion to determine the efficiency of the design optimization algorithm [1, 3, 4].

Mathematically, the general form of an optimization problem is as follows:

$$\text{Minimize } f(x) \quad (9)$$

$$\text{Subjected to: } h_i(x) \leq 0, i = 1, \dots, m_{IE} \quad (10)$$

$$g_i(x) = 0, i = 1, \dots, m_{EQ} \quad (11)$$

$$x_L \leq x \leq x_U$$

In Eqs. (9)-(11),  $f(x)$  is an objective function,  $h(x)$  and  $g(x)$  are constraint functions,  $x$  is the vector of the design variables,  $x_L$  and  $x_U$  are the lower and upper limits of  $x$ ,  $m_{IE}$  and  $m_{EQ}$  are the number of inequality constraint conditions and the number of equality constraint conditions respectively.

The sequential quadratic programming (SQP) method is a very effective technique that can be used to solve a nonlinear constrained optimization problem, and it is well-suited to solve problems that have significant nonlinearity, such as the hull-form optimization problem.

We write the Lagrangian for the optimization problem as follows:

$$\mathcal{L}(x, \lambda, \sigma) = f(x) - \lambda^T b(x) - \sigma^T c(x) \quad (12)$$

In Eq. (12),  $\lambda$  and  $\sigma$  are the Lagrangian multipliers. For an iterate  $x_k$ , a basic sequential quadratic programming algorithm defines the appropriate search direction  $d_k$  as the solution to the quadratic programming sub-problem.

$$\text{Minimize } f(x_k) + \nabla f(x_k)^T d + \frac{1}{2} d^T \nabla_{xx}^2 \mathcal{L}(x_k, \lambda_k, \sigma_k) d \quad (13)$$

$$\text{Subjected to: } h(x_k) + \nabla h(x_k)^T d \geq 0 \quad (14)$$

$$g(x_k) + \nabla h g(x_k)^T d \geq 0 \quad (15)$$

#### 4. Evaluation of objective function

The external flows around the bodies can be treated as inviscid and irrotational since the viscous effects are limited to a thin layer next to the body, which is called the boundary layer. A potential function,  $\phi(x, y, z, t)$ , could be defined as a continuous function that satisfies the conservation of mass and momentum, assuming incompressible, inviscid and irrotational flow. A velocity vector in the flow field around the body could be defined as the gradient of the potential function [2].

$$\vec{V} = \nabla \phi \quad (16)$$

The velocity must still satisfy the conservation of mass equation. We can substitute the relationship between the potential and the velocity to arrive at the Laplace Equation that is used as the governing equation in the present study.

$$\nabla^2 \phi = 0 \quad (17)$$

Over the wetted part of the hull surface, the velocity potential must satisfy the hull boundary condition of zero flow normal to the surface.

$$\phi_n = 0 \quad (18)$$

$n$  : Unit normal vector to the hull surface

The radiation condition must be satisfied, as follows:

$$\nabla \phi \rightarrow (U_{ship}, 0, 0) \text{ as } x^2 + y^2 + z^2 \rightarrow \infty \quad (19)$$

$U_{ship}$  : Advance speed of a ship

On the free surface, the kinematic and dynamic conditions must be satisfied according to the following equations:

$$\phi_x \eta_x + \phi_y \eta_y - \phi_z = 0 \text{ on } z = \eta \quad (20)$$

$$\eta = \frac{1}{2g} (U_{ship}^2 + \nabla \phi \cdot \nabla \phi)$$

$g$ : Gravitational acceleration

The potential based panel method is used to obtain  $\phi$  in Eq. (20), and the nonlinearity in Eq. (20) is solved by applying the iterative approach after the linearization with Eq. (20). In each iteration step, the calculation panels for the hull surface are generated by applying the panel cutting method, and the trim and sinkage of the ship are taken into account.

Having obtained the velocity potential and the flow velocity, the pressure coefficient ( $C_p$ ) for each panel can be determined according to Bernoulli's equation.

$$C_P = 1 - \frac{\nabla\phi \cdot \nabla\phi}{U_{ship}^2} - 2 \frac{z}{Fn^2} \quad (21)$$

$Fn$ : Froude number

The wave making resistance coefficient ( $C_W$ ) is then given using the pressure integral over the wetted hull surface, and the wave making resistance coefficient is used as an objective function of the hull form optimization problem.

$$C_W = - \frac{\int_S C_P n_x ds}{S} \quad (22)$$

$n_x$  : x –component of unit normal vector to the hull surface

$S$  : Wetted surface area of the hull surface

## 5. Application

A passenger ship had been selected in order to verify the effectiveness of the proposed hull-form optimization algorithm. Fig. 12 and Table 1 show the main dimensions and body plan of the passenger ship, and a model test was performed in the towing tank in order to verify the validity of the applied numerical flow analysis solver [9].

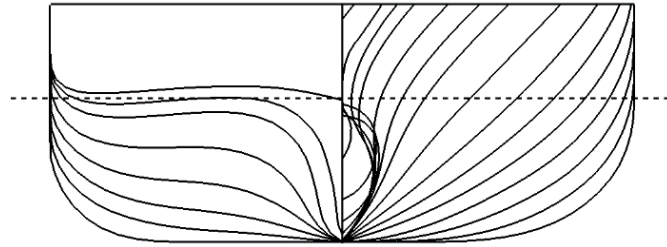


**Fig. 12** Lines of the passenger ship

**Table 1** Main dimensions of the passenger ship

Designation	Symbol	Ship	Model
Scale Ratio	$\lambda$	26.0	
Design Speed	$Fn$	0.340	
Length Overall	LOA (m)	157.0	6.038
Length Between Perpendicular	LBP (m)	144.0	5.538
Breadth	B (m)	24.60	0.946
Depth	D (m)	14.50	0.558
Draft	T (m)	6.00	0.230
Displacement	$\nabla$ (m <sup>3</sup> )	12,123	0.690
Wetted Surface Area	$S_{WET}$ (m <sup>2</sup> )	3,781	5.592
Block Coefficient	$C_B$	0.57	

### 5.1 Design Variables

Ship optimization was performed for the region extending about 25% of the ship's length from the bow as shown in Fig. 13, wherein the flow might be assumed to be the potential flow.



**Fig. 13** Region to be optimized for the passenger ship

Fig. 14 shows 3 design variables (blue points) that could move  $\pm 1$  meter to the normal vector direction of the original hull profile, as shown in Eq. (23).



**Fig. 14** Design variables used to modify the hull profile

$$-1 \text{ m} \leq \alpha \leq +1 \text{ m} \quad (23)$$

Fig. 15 shows 10 design variables (red points) that could move  $\pm 1$  meter in the transverse direction, as shown in Eq. (24).

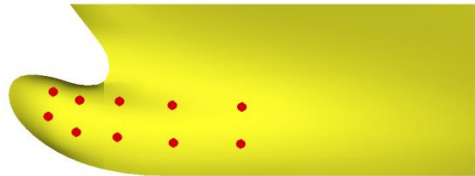


**Fig. 15** Design variables used to modify the hull surface

$$-1 \text{ m} \leq \alpha \leq +1 \text{ m} \quad (24)$$

### 5.2 Constraint conditions

The constraint conditions of the volume displacement and the wetted surface area of the ship are prescribed by the ship designer, and these are the most important factors in the hull form design.

The constraints for the volume displacement ( $\nabla$ ) and the wetted surface area ( $S_{WET}$ ) were set as follows.

$$\nabla \geq \nabla_{original \text{ hull}} \quad (25)$$

$$S_{WET} \geq S_{WET \text{ original hull}} \quad (26)$$

A constraint was applied for the normal vector to the hull surface to avoid the evolution of the hull in an undesirable direction as shown in Fig. 16.

$$n_x \leq 0.1736 \quad (27)$$

$n_x$  : x-component of the unit vector normal to the hull surface

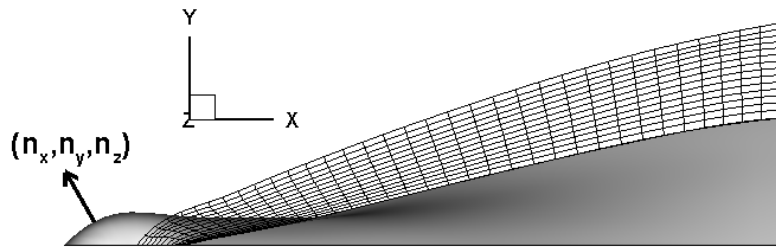


**Fig. 16** Definition of the normal vector

### 5.3 Computational results

The numerical analysis is performed to optimize the hull-form of the passenger ship at the design speed ( $F_n = 0.340$ ), and the number of panels used in the numerical analysis is 7122, distributed on the free surface (3440) and on the hull surface (3682).

The body plans and the sheer plans of the original hull and the optimized hull are shown in Figs. 17 and 18, and the sectional-area curves are compared in Fig. 19. As shown in Figs. 17–19, the bulbous bow of the optimized hull is modified in shape in order to pass through the free surface, and it is bigger and longer when compared to the bulbous bow of the original hull.

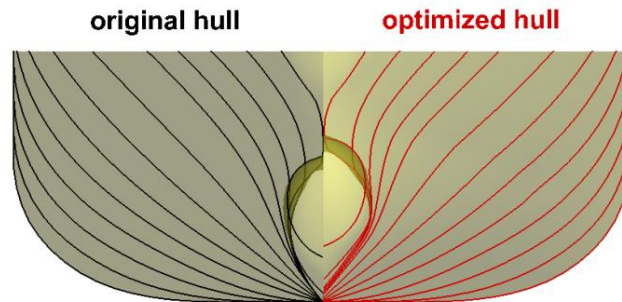


**Fig. 17** Comparison of the body plans

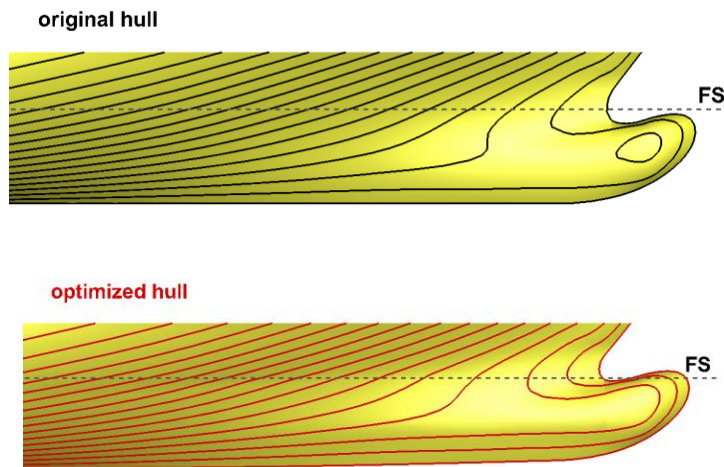


**Fig. 18** Comparison of the bow-part sheer plans

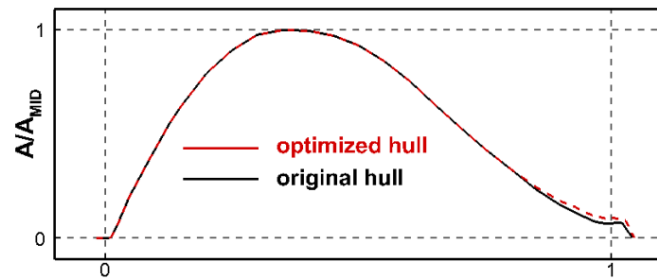


Fig. 19 Comparison of the sectional-area curves

In Fig. 20, the wave heights of the optimized hull are compared to those of the original hull in the longitudinal direction at  $y/L_{BP} = 0.10$  and  $0.14$  m. The wave heights of the optimized hull were reduced near the bow part in comparison with those of the original hull.

In Fig. 21, the wave pattern of the optimized hull is compared with that of the original hull, and the wave height decreased over the entire free-surface area.

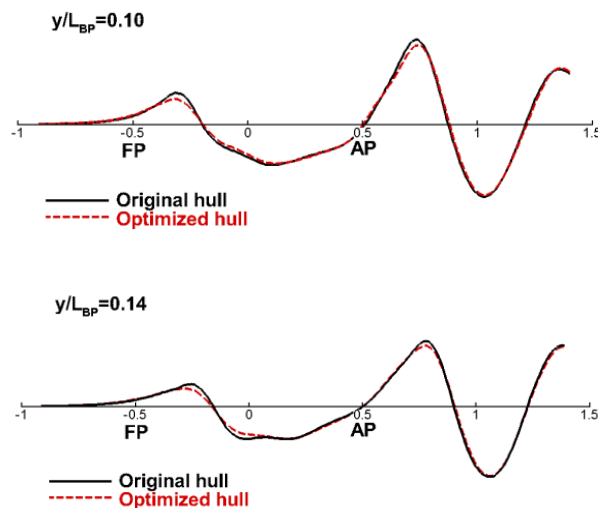


Fig. 20 Comparison of the wave heights

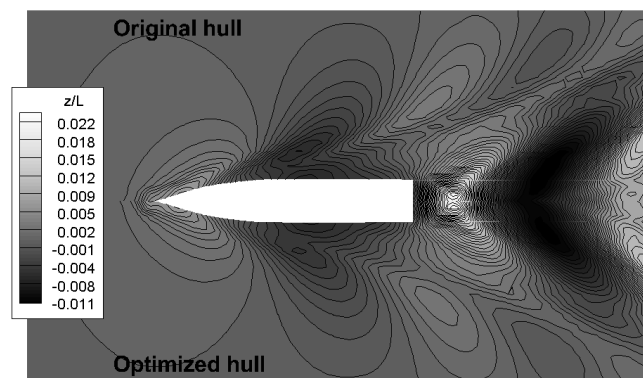


Fig. 21 Comparison of the wave patterns

Table 2 compares the volume displacement, the wetted surface area, and the wave-making resistance of the optimized hull with those of the original hull. The volume displacement and the wetted surface area of the optimized hull very slightly increased, and the wave-making resistance of the optimized hull was reduced by about 12%.

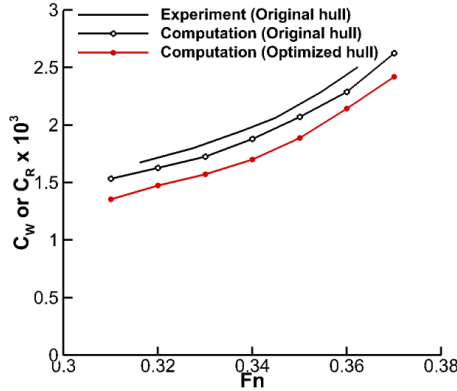


Fig. 22 Comparison of the residual/wave-making resistance coefficients

Table 2 Comparison of the hydrostatic data and the wave-making resistance

	Original	Optimized	$\Delta$ (%)
$\nabla$ (displacement) (m <sup>3</sup> )	12,123	12,212	+0.740
$S_{WET}$ (m <sup>2</sup> )	3,781	3,797	+0.043
$C_W \times 10^3$	1.85602	1.64010	-11.63

Fig. 22 compares the wave-making-resistance coefficient, and the residual-resistance coefficient (solid line without symbol, black;  $C_R$ ) was measured by conducting a model test that was performed for the original hull in order to verify the validity of the applied numerical flow analysis solver. In the towing-tank experiment, studs were attached to the hull surface as turbulence simulators in the middle of the bulbous bow, and the trim and sinkage of the model were taken into account. As indicated with Fig. 22, the results for the original hull that were calculated by the numerical analysis well predicted the results measured by the model test over the entire speed region.

The wave-making resistance of the optimized hull was thus reduced by about 12 % when compared to the original hull at the design speed.

## 6. Conclusions

The present study proposes an automatic hull form control algorithm that adopts a Gaussian distribution function to efficiently control the hull form of a ship during hull form optimization. A numerical analysis was then performed for the hull form optimization by applying proposed algorithm with a passenger ship.

The results of the numerical analysis between the original hull and the optimized hull indicate that the numerical technique that was developed to efficiently control the hull form and to identify the ship with the minimum wave-making resistance is reliable and helpful in improving the wave-making-resistance performance of ships.

## REFERENCES

- [1] Choi, H.-J., "Hull-form optimization of a container ship based on bell-shaped modification function," *International Journal of Naval Architecture and Ocean Engineering*, Vol. 7, No. 3, pp. 478-489 (2015). <http://dx.doi.org/10.1515/ijnaoe-2015-0034>.
- [2] Choi, H.-J., Chun, H.-H., Park, I.-L. and Kim, J., "Panel cutting method: new approach to generate panels on a hull in Rankine source potential approximation," *International Journal of Naval Architecture and Ocean Engineering*, Vol. 3, pp. 225-232 (2011). <http://dx.doi.org/10.3744/JNAOE.2011.3.4.225>.
- [3] Choi, H.-J., Park, D.-W. and Choi, M.-S., "Study on optimized hull form of basic ships using optimization algorithm," *Journal of Marine Science and Technology*, Vol. 20, No. 1, pp. 60-68 (2015).
- [4] Frank, E.-C. and Michael, L.-O., "A sequential quadratic programming algorithm for nonconvex, nonsmooth constrained optimization," *Journal of Society for Industrial and Applied Mathematics*, Vol. 22, No. 2, pp. 474-500 (2012).
- [5] Grigoropoulos, G.-J., "Hull form optimization for hydrodynamic performance," *Marine Technology*, Vol. 41, No. 4, pp. 167-182 (2004).
- [6] Han, S.-H., Lee, Y.-S. and Choi, Y.-B., "Hydrodynamic hull form optimization using parametric models," *Journal of Marine Science and Technology*, Vol. 17, pp. 1-17 (2012). <http://dx.doi.org/10.1007/s00773-011-0148-8>.
- [7] Jeong, S.-K. and Kim, H.-Y., "Development of an efficient hull form design exploration framework," *Mathematical Problems in Engineering*, Volume 2013, Article ID 838354, 12 pages (2013).
- [8] Kim, H.-Y., Yang, C. and Noblesse, F., "Hull form optimization of reduced resistance and improved seakeeping via practical design-oriented CFD tool," In *Proceedings of the Grand Challenges in Modeling and Simulation Conference*, pp. 375-385 (2010).
- [9] Lee, G.-H., Kim, J.-H., Jang, H.-S., Joo, Y.-R. and Chun, H.-H., "Development of Medium Size High Speed Ro-Pax Vessel," *Journal of the Society of Naval Architects of Korea*, Vol. 41, No. 1, pp. 64-69 (2004) (in Korean). <http://dx.doi.org/10.3744/SNAK.2004.41.1.064>.
- [10] Suzuki, K., Kai, H. and Kashiwabara, S., "Studies on the optimization of stern hull form based on a potential flow solver," *Journal of Marine Science and Technology*, Vol. 10, No. 2, pp. 61-69 (2005). <http://dx.doi.org/10.1007/s00773-005-0198-x>.
- [11] Zhang, B.J., "Research on optimization of hull lines for minimum resistance based on Rankine source method," *Journal of Marine Science and Technology*, Vol. 20, No. 1, pp. 89-94 (2012).
- [12] Zhang, B.J., "The optimization of the hull form with the minimum wave making resistance based on Rankine source method," *Journal of Hydrodynamics*, Vol. 21, No. 2, pp. 277-284 (2009). [http://dx.doi.org/10.1016/S1001-6058\(08\)60146-8](http://dx.doi.org/10.1016/S1001-6058(08)60146-8).

Submitted: 08.01.2016.

Accepted: 10.03.2016.

Hee-Jong Choi, choihj@jnu.ac.kr

Department of Naval Architecture & Ocean Engineering,  
Chonnam National University, Yeosu, South Korea

Hyun-Sik Yoon

Global Core Research Centre of Ships and Offshore Platforms,  
Pusan National University, Busan, South Korea